SAND--96-8494C
CONF-960772--4

Flickering Frequency and NO_X and CO Emission Indexes of an Unsteady Laminar Diffusion Flame for Varying Gravitational Force Using a Flamelet Model

Clement G. Yam
Combustion Research Facility
Sandia National Laboratories
Livermore, CA 94551-0969
U. S. A.
Tel: (510) 294-2930
Fax: (510) 294-1004
e-mail: cgyam@ca.sandia.gov

Kenneth D. Marx
Combustion Research Facility
Sandia National Laboratories
Livermore, CA 94551-0969
U. S. A.
Tel: (510) 294-2441
Fax: (510) 294-1004
e-mail: marx@ca.sandia.gov

Jyh -Yung Chen
Mechanical Engineering Department
University of California, Berkeley
Berkeley, CA 94720
U. S. A.
Tel: (510) 642-3286
Fax: (510) 642-6163
e-mail: jychen@firebug.berkeley.edu

Chen Pang Chou
Mechanical Engineering Department
University of California, Berkeley
Berkeley, CA 94720
U. S. A.
Tel: (510) 643-6506
Fax: (510) 642-6163
e-mail: cpchou@firebug.berkeley.edu

Total word counts:		5848
Words:		3881
Equations:	17x21=	357
Figures + Table:	8x200=	1600

Authors' preference for oral presentation.
Topic area=Laminar Flames

Flickering Frequency and NO_X and CO Emission Indexes of an Unsteady Laminar Diffusion Flame for Varying Gravitational Force Using a Flamelet Model

Clement G.Yam[1], Kenneth D. Marx[1], Jyh-Yuan Chen[2] and Chen-Pang Chou[2]

Abstract

The effects of varying gravitational force on the natural flickering frequency and on the emission indexes of NO_X and CO of an unsteady laminar methane diffusion flame are investigated numerically. A second-order time-accurate numerical scheme is developed for solving the transient Navier-Stokes equations with the low Mach number formulation. With the flamelet model, this numerical scheme provides an efficient tool for studying transient flame behavior. The computed flickering frequencies exhibit an approximate inverse square root dependence on Froude number. A linear stability analysis is performed to gain insight into the physical nature of the flickering behavior. The numerical model predicts a strong influence of gravitational force on instantaneous and time-averaged emission indexes of NO_X and CO.

Introduction

Accurate numerical simulation of low Mach number unsteady flows is a challenging task due to the stiffness caused by acoustic waves. When coupled with chemical reactions, the flow is further characterized by multiple time and spatial scales associated with chemical kinetics. Not only does one need to resolve the fluid time scale, but it is also necessary to resolve the widely-spread chemical time scales. For fuels involving fast chemistry, the equilibrium flame sheet model can be used to avoid solving the energy and species equations [1]. However, the equilibrium flame sheet model is inaccurate for predicting NO_X and CO emissions for flames with short residence times. Reduced mechanisms can be used to cut down the computer time and memory demands; however, stiffness in chemical kinetics often severely restricts the size of the time step; therefore the time saving is limited.

In this study, the flamelet approach traditionally implemented for modeling turbulent combustion (see, e.g., Peters [2]) is extended to transient laminar flames with NO_X formation. For diffusion flames, a flamelet library in terms of mixture fraction f and its scalar dissipation rate χ is constructed with detailed chemistry prior to the flow field calculation. This flamelet library provides thermochemical properties needed in the flow field calculation, such as density ρ, mixture viscosity μ, and mixture diffusivity D. The combustion and fluid flow is coupled directly by solving for the mixture fraction field using these properties and computing the scalar dissipation rate from the resulting mixture fraction field. During the computation, the continuity equation and the momentum equations are solved simultaneously with the mixture fraction. The

[1] Combustion Research Facility, Sandia National Laboratories, Livermore, California
[2] University of California, Berkeley

thermochemical properties are evaluated as a function of f and χ by bilinear interpolation from the flamelet library. The source terms for NO_X species, NO and NO_2, are determined from the flame temperature and species concentrations from the library.

Previous numerical simulations of unsteady flames have often been initialized with a uniform flow field within the domain of interest [4, 5]. Variations in temperature and density are then slowly introduced into the simulation. Although this suffices to determine the flickering frequency of the flame, this type of calculation avoids the temporal development of the flame, which is difficult to simulate. This is because the velocity field has an initial value of zero magnitude everywhere, and the system is subject to a rapid change in density (e.g., by a factor of seven) resulting from the flame front propagating downstream. The present numerical scheme has been shown to be accurate and stable enough to solve for rapid changes in the flow field. The present study simulates the first ten seconds of the formation of a small methane jet diffusion flame exhibiting the rapid expansion of a hot reacting jet injected into a cold still air environment. The ability to simulate the early formation of this expanding reacting jet indicates that the method employed is stable and robust enough to study various kinds of unsteady reacting flows.

The origin of the oscillation of this and similar flames is the Kelvin-Helmholtz instability which occurs because of the shear between the rapidly rising hot gases and the cold surrounding air. After a discussion of the results of the numerical simulation of the flame, we present an approximate analysis of this instability, and show that it permits a crude estimate of the flickering frequency.

Problem of Interest

The numerical model is used to simulate the unsteady laminar methane jet diffusion flame investigated experimentally by Smyth et al. [5]. The experiments used a co-annular axisymmetric burner with a fuel diameter of 1.1 cm surrounded by an annulus of coflowing air with an outer diameter of 10.2 cm. Both the fuel jet and the coflow air velocities are maintained at 7.9 cm/s. The computational domain covers a region of outer radius of 20 cm and an axial distance of 45 cm. A total of 52 by 122 grid points in the radial and axial directions, respectively, are used. Numerical results for the flame height in the quasisteady state, the natural flickering frequency, and emission indexes for NO_X and CO under various magnitudes of gravitational force will be discussed.

Governing Equations

For solving low speed subsonic flows, we adopt an approach which splits the pressure field into thermodynamic pressure and the dynamic pressure [6, 7]

$$P_{Total} = P_{Thermal} + P_{Dynamic} \tag{1}$$

with

$$P_{Thermal} = \rho RT. \tag{2}$$

Using this decomposition of pressure field, the following time-dependent governing equations can be derived for low Mach number flows:

I. Continuity Equation:

$$\frac{\partial \rho}{\partial t} + \vec{\nabla} \bullet (\rho \vec{V}) = 0, \tag{3}$$

where ρ is density, t is time, and $\vec{V}$ is the velocity vector.

II. Momentum Equation:

$$\rho \frac{\partial \vec{V}}{\partial t} + \rho \vec{V} \bullet \vec{\nabla} \vec{V} = -\vec{\nabla} P + \vec{\nabla} \bullet \vec{\tau} + \rho \vec{g}, \tag{4}$$

where P is the dynamic pressure, $\vec{g}$ is the gravitational vector, and $\vec{\tau}$ is the stress tensor:

$$\tau_{ij} = \mu \left(\frac{\partial u_i}{\partial x_j} + \frac{\partial u_j}{\partial x_i} - \frac{2}{3} \delta_{ij} \vec{\nabla} \bullet \vec{V} \right). \tag{5}$$

III. Mixture Fraction Equation:

$$\rho \frac{\partial f}{\partial t} + \rho \vec{V} \bullet \vec{\nabla} f = \vec{\nabla} \bullet (\rho D \vec{\nabla} f), \tag{6}$$

where f is the mixture fraction and D is the mixture diffusion coefficient.

IV. Equation for the mass fraction of NO and NO_2:

$$\rho \frac{\partial Y_k}{\partial t} + \rho \vec{V} \bullet \vec{\nabla} Y_k = \vec{\nabla} \bullet (\rho D_k \vec{\nabla} Y_k) + \dot{\omega}_k, \tag{7}$$

where Y_k is the mass fraction of species k, D_k is the diffusion coefficient, and $\dot{\omega}_k$ is the chemical source term.

Flamelet model

A detailed description of the laminar flamelet method for the turbulent flow simulation

can be found in the review paper by Peters [2]. The flamelet library concept preserves the essential idea of the flame sheet model, i.e., the independence of the flow field and the chemistry. Instead of assuming the flame to be at the equilibrium state, the flamelet approach introduces a parameter, the scalar dissipation rate, to describe the departure of the chemical kinetics from equilibrium. Following the approach described in [2], one can transform the energy and the species equations from the original spatial coordinate system (t,x_1,x_2) to a coordinate system attached to the surface of constant mixture fraction (t, f, x_2). The flamelet theory assumes that derivatives with respect to x_2 are of lower order compared to the derivatives with respect to f when the reaction zone is thin, i.e., $\frac{\partial}{\partial f} >> \frac{\partial}{\partial x_2}$. With this assumption, one can derive the following equations for species and temperature:

Species Equation :

$$\rho \frac{\partial Y_k}{\partial t} = \rho \frac{D_k}{D} \frac{\chi}{2} \frac{\partial^2 Y_k}{\partial f^2} + \dot{\omega}_k \tag{8}$$

Energy Equation :

$$\rho \frac{\partial T}{\partial t} = \rho Le \frac{\chi}{2} \frac{\partial^2 T}{\partial f^2} - \sum_k \frac{\rho \dot{\omega}_k h_k}{\overline{Cp}} \tag{9}$$

where h_k is the enthalpy of species k, $\overline{Cp}$ is the average specific heat of the mixture, Le is the Lewis number, $Le = \frac{\lambda}{\rho D \overline{Cp}}$, λ is the thermal diffusivity, and the scalar dissipation rate is defined as $\chi = 2\nabla f \cdot \nabla f$. The scalar dissipation rate may be interpreted either as the inverse of a characteristic diffusion time or as a quantity related to the strain rate imposed on the flame. By assigning different values of χ, equations (8) and (9) can be solved with detailed chemistry to construct the library file. These stiff equations are solved by Newton iteration with local grid refinement.

Numerical Method

A semi-explicit scheme which is second-order in both space and time is used in this study. It is a modified version of the solution scheme devised by Kim and Moin [8]. A detailed discussion of the pressure solver, special treatment of the mixture fraction equation, the initial and boundary conditions, and the stability criteria are given in Yam, et al. [9,10].

The mass fraction equations for pollutant species NO and NO_2 are solved using the basic scheme of Kim and Moin [8]. The chemical source terms are determined from the thermochemical terms in the flamelet library. Using detailed chemistry with the assumption that N atom is in steady state, the chemical source terms are given in the form

$$\dot{\omega}_{NO} = a_1 - b_1 \cdot Y_{NO} + c_1 \cdot Y_{NO_2} \tag{10}$$

$$\dot{\omega}_{NO_2} = a_2 + b_2 \cdot Y_{NO} - c_2 \cdot Y_{NO_2}, \tag{11}$$

where a_1, a_2, b_1, b_2, c_1 and c_2 are coefficients obtained from the flamelet library.

Discussion of results

I) Results for the 1 g case

To demonstrate the robustness of the present numerical code, the simulation is started with simultaneous injections of both fuel and coflowing air into initially quiescent air. Combustion is assumed to initiate in regions near stoichiometric. Figure 1 presents the predicted maximum temperature location for the first ten seconds. As seen in this figure, during the first four seconds, the flame height oscillates dramatically in response to sudden changes in density and velocity. As the flame evolves further in time, a repeating flickering behavior starts to emerge. This motion results from an instability generated by the shearing action between the buoyancy-driven burned gases and the surrounding cold air leading to a well-characterized frequency. The computed characteristics of such a flickering flame will be analyzed only after the initial transient subsides. The flickering frequency is determined to be 12.6 Hz, which is in close agreement with the frequency of 12 Hz measured by Smyth, et al. [5]. After the diffusion flame reaches a quasisteady state, it exhibits an average flame height of about 59 mm based on temperature profiles. This stoichiometric flame height is shorter than the visible flame height of 79 mm based on the OH and soot images measured by Smyth, et al. [5]. Visible flame height based on light emission is known to be longer than the stoichiometric flame height. The ratio between the predicted stoichiometric flame height and the visible flame height is 0.75. This value is surprisingly close to the ratio observed experimentally in turbulent hydrogen flames by Barlow and Carter [11].

The emission indexes of NO_X and CO are reported as a function of time at the outflow boundary plane (45 cm from the jet exit plane). Following convention, the emission index of NO_X is defined as:

$$EI_{NO_X} = \frac{1}{Y_{fuel}} \frac{1}{\dot{M}_{fuel}} \left[\frac{MW_{NO_2}}{MW_{NO}} \dot{M}_{NO} + \dot{M}_{NO_2} \right], \tag{12}$$

where $\dot{M}$ is the mass flow rate, MW is the molecular weight, and Y is the mass fraction.

The emission index of CO is defined as:

$$EI_{CO} = \frac{1}{Y_{fuel}} \frac{1}{\dot{M}_{fuel}} \left[\dot{M}_{CO} \right]. \tag{13}$$

As shown in Fig. 2, the emission index of NO_X (EI_{NOX}) starts to grow after an elapsed time of 0.35 seconds. This is the time required to propagate to the exit plane. The value of EI_{NOX} exhibits a high peak of 4 g/Kg and then drops back to 0.6 g/Kg. This is due to the formation of an initial flame front with a much larger diameter than the fully developed flame diameter, resulting in a higher emission index than that for the fully developed flame. The value of EI_{NOX} continues to exhibit chaotic fluctuations up to a time of 4 seconds, when the fluctuations start to repeat. The mean EI_{NOX} is 1.30 g/Kg. A similar analysis for the emission index of CO (EI_{CO}) (Fig. 3) is also performed. The mean EI_{CO} is determined to be 65.4 g/Kg.

Closer inspection of the instantaneous emission indexes for NO_X and CO indicates that the oscillations are also in phase. This is because the emission indexes are determined at the exit plane. As the fluid containing the burned gases exits the domain, the amount of NO_X and CO are determined simultaneously across that plane. Further study of the entire instantaneous flame structure indicated that locally, those regions which have maximum concentration of NO_X have minimum CO concentration.

II) Summary of the four cases in this study

Three additional simulations with different g values have been performed under the same inflow and outflow conditions as in the 1 g case. Table 1 summarizes the predicted characteristics versus the magnitude of gravity and the Froude number ($Fr=W^2/(gD)$, where W is the mean fuel exit velocity, D is the fuel jet diameter).

Table 1
Summary of time-averaged statistics.

G-Force	Froude Number	f (Hz)	$\overline{X_{T\max}}$ (cm)	$\overline{EI_{NOx}}$ (g/Kg)	$\overline{EI_{co}}$ (g/Kg)	$\overline{\chi}$ (1/s)	$\overline{\chi}_f$ (1/s)
0.1 g	0.0578	3.62	5.08	2.02	53.6	0.218	0.0725
0.5 g	0.0116	8.45	5.52	1.47	58.5	0.249	0.119
1.0 g	5.78e-3	12.3	5.89	1.30	65.4	0.277	0.182
2.0 g	2.89e-3	19.6	6.35	1.07	72.9	0.315	0.223

Mean and conditional scalar dissipation rates over the entire computational domain are included in the table to provide insights into the computed emission characteristics. The mean scalar dissipation rate is estimated by

$$\overline{\chi} = \frac{1}{\tau}\int_{t0}^{t0+\tau} \frac{1}{N}\sum_{i=1}^{N} \chi_i d\tau, \qquad (14)$$

where τ is the period for one cycle, N is the total number of grid points, and χ_i is the scalar dissipation rate at each grid point. The conditional scalar dissipation rate is computed by

$$\overline{\chi}_{\mathrm{f}} = \frac{1}{\tau}\int_{t0}^{t0+\tau} \frac{1}{N}\sum_{i=1}^{N} \chi_i \cdot I \, d\tau, \qquad (15)$$

where I=1 when the mixture fraction lies between 0.04 to 0.07 and I=0 otherwise.

As revealed in Table 1, the predicted flickering frequency increases by a factor of 5.5 when the gravitational force increases twenty-fold. The effect of gravity on the mean flame height is less; only a 20% increase is observed over the range 0.1g to 2.0g. The results also reveal that as the gravitational force increases, the mean EI_{NOX} decreases while the mean EI_{CO} increases. By correlating the predicted flickering frequency, emission indexes for NO_X and CO, mean and conditional dissipation rates with the Froude number as shown in Figs. 4, 5 and 6, we obtain the following scaling relationships: $f \sim \mathrm{Fr}^{-0.56}$, $EI_{NOX} \sim \mathrm{Fr}^{0.21}$, $EI_{CO} \sim \mathrm{Fr}^{-0.10}$, $\overline{\chi} \sim \mathrm{Fr}^{-0.12}$, and $\overline{\chi}_{\mathrm{f}} \sim \mathrm{Fr}^{-0.38}$.

These relations are approximate as they are based on only four points; however, they exhibit interesting features as discussed below. As the gravitational force decreases, (Fr increases), the gradient of the mixture fraction between the hot gases and the cold surrounding air decreases. Consequently, the scalar dissipation rate decreases with the Froude number. It is interesting to note that the predicted $\overline{\chi}_{\mathrm{f}} \sim \mathrm{Fr}^{-0.38}$ has a negative dependence on Fr similar to the scaling relation, $\overline{\chi}_{\mathrm{f}} \sim 3(g/D)^{0.5}\mathrm{Fr}^{-0.1} \sim 3W/D\ \mathrm{Fr}^{-0.6}$, suggested for buoyancy-controlled turbulent jet flames [12]. Since CO is not computed kinetically, EI_{CO} is determined by the scalar dissipation field. For small variation in χ, CO changes with χ approximately linearly. This leads to $EI_{CO} \sim \overline{\chi} \sim \mathrm{Fr}^{-0.12}$, which agrees with the computed scaling, $EI_{CO} \sim \mathrm{Fr}^{-0.10}$. Based on the asymptotic analysis by Rokke, et al. [12], the prompt and Zeldovich NO sources, when integrated over the mixture fraction space, have the following dependence on the scalar dissipation rate, $\hat{\omega}_{\mathrm{prompt}} \approx 1.4x10^{-7}\chi_f^{7/8}$, $\hat{\omega}_{\mathrm{Zeldovish}} \approx 3.x10^{-7}\chi_f^{-0.4}$, where χ_{f} is the scalar dissipation rate at the stoichiometric. Since the computed χ_f values under the present conditions are below 1, the dominant contribution of NO arises via the Zeldovich route. Under this condition, EI_{NOX} is expected to scale with $\chi_f^{-0.4}$ leading to $EI_{NOX} \sim (\overline{\chi}_{\mathrm{f}})^{-0.4} \sim (\mathrm{Fr}^{-0.38})^{-0.4} \sim \mathrm{Fr}^{0.15}$. An alternative way to estimate the dependence of EI_{NOX} on χ_f is based on the computed EI_{NOX} for a series of one-dimensional opposed stagnation flames reported by Yamashita, et al. [13]. Their results indicate that $EI_{NOX} \sim \chi_f^{-0.5}$ over a range of χ_f from 0.17 to 5. Using this relation, we obtain a scaling relation $EI_{NOX} \sim \mathrm{Fr}^{0.19}$. Both of these estimates give a positive power dependence of EI_{NOX} on Fr, a trend consistent with the computed scaling relation. The estimated exponent is in the range of 0.15 to 0.19 which is close to the computed value of 0.21. The above analysis suggests that the computed buoyantly unstable flames exhibit characteristics markedly similar to those from buoyancy-controlled turbulent jet flames.

Approximate Flow Instability Analysis

The question of the origin of flame oscillation has been studied by a number of researchers

(see References 14-16 and the works cited therein). Buckmaster and Peters [15] develop a similarity solution to a system of boundary-layer equations which describe the flow associated with a flame sheet. Mahalingam, et al. [16] obtain solutions for parallel flow which includes heat release due to chemical reactions. Their treatment includes premixed and nonpremixed flames, and allows for three-dimensional perturbations

The mechanism for the oscillation is the Kelvin-Helmholtz instability [14-16]. The conditions for such an instability exist in the diffusion flame because a jet of reactants and products passes through the slower coflowing air. The vorticity in our calculations (e.g., Fig. 7) exhibits the expected vortex rollup near the flame and a more complex evolution downstream.

We have not undertaken an analysis as broad as those given in References 15 and 16. Our consideration is limited to the particular laminar diffusion flame discussed here. In order to apply the theory of the Kelvin-Helmholtz type of instability to this flame, we need to determine appropriate velocity and density profiles. We adopt the usual approach of assuming an unperturbed flow that is approximately uniform in the axial (vertical) direction. This is not a particularly good assumption on the scale of the axial variation in the perturbed flow of interest, so we must make a choice. Inspection of the computational results indicates that most of the action occurs in the range 5 cm $\le z \le$ 10 cm. We therefore make the somewhat arbitrary choice of $z = 7.5$ cm as the point at which to obtain the profiles that we use for the unperturbed flow. A piecewise linear approximation is used in which the velocity is $w_{01} = 255$ cm/s in a core of radius a=0.4 cm, makes a linear transition to $w_{02} = 5.0$ cm/s at radius b=1.4 cm, and remains constant thereafter. The density is assumed constant at ρ_1=0.24 g/cm^3 for $r<b$ and ρ_2=1.17 g/cm^3 for $r>b$.

Assuming an unperturbed flow uniform in the axial direction, we look for axisymmetric modes of the form $\exp[i(kz-\omega t)]$. Since we seek only order-of-magnitude approximations and scaling laws, we assume slab geometry instead of the more appropriate axisymmetric cylindrical coordinates. Following the usual procedures [15-17], we obtain the following dispersion relation connecting the frequency and wave number for inviscid perturbations:

$$[(\nu-\eta)(\coth\eta\alpha+1)-\gamma][(\nu-\eta\beta)(\sigma+1)+\gamma]$$
$$-[(\nu-\eta)(\coth\eta\alpha-1)-\gamma][(\nu-\eta\beta)(\sigma-1)+\gamma]e^{-2\eta\delta}=0 \qquad (16)$$

The dimensionless quantities appearing here are defined as follows: frequency $\nu=b\omega/w_{01}$, wave number $\eta=kb$, core radius $\alpha=a/b$, width of transition region $\delta=(b-a)/b$, coflow velocity $\beta=w_{02}/w_{01}$, transition velocity gradient $\gamma=(\beta-1)/\delta$, and density ratio $\sigma=\rho_2/\rho_1$.

The approach taken is to look for waves which propagate upwards and are amplified in the upward direction. To this end, we solve (16) numerically for complex wave number as a function of real frequency. The frequency at which the spatial growth rate $Im(\eta)$ is a maximum is taken as the frequency of oscillation of the flickering flame [15, 16]. For our 1 g case, this

frequency is 5.85 Hz, approximately half the actual value obtained from the full simulation. However, it should be noted that this value is very sensitive to the width of the transition region, and is therefore sensitive to the choice of profile discussed above. It should be regarded only as an order-of-magnitude estimate.

We now consider the variation of the flicker frequency with the magnitude of the gravitational acceleration. Up to this point, g has not entered into the equations for the perturbed quantities. It plays a role only in accelerating the hot gases upwards, thereby increasing the velocity w_{01} used in the stability analysis. A crude one-dimensional approach to calculating the velocity of the unperturbed flow yields

$$w_{01} = \sqrt{w_j^2 + 2\left(\frac{\rho_2}{\rho_1} - 1\right)gz} \tag{17}$$

where w_j is the velocity at the jet orifice (z=0). Assuming z=7.5 cm as discussed above, values of g corresponding to the Froude numbers used above were used to obtain appropriate velocities w_{01}. The resulting frequencies are plotted in Fig. 4. It is seen that the calculated frequency is very nearly proportional to $Fr^{-0.5}$. This is predictable from the fact that $\beta=w_{02}/w_{01}$ and w_j/w_{01} are both small; in the limit that these two quantities go to zero it is easily seen that Eq. (16) need only be solved once for given values of δ and σ. Then f scales as w_{01}/b, and w_{01} scales as $g^{0.5}$.

The lack of quantitative agreement with the two-dimensional simulation is due to the following defects in the stability analysis: (1) Rectangular geometry is used instead of cylindrical coordinates. (2) The assumption of axial invariance of the unperturbed configuration is not well-justified. (3) The analysis involves the inviscid linearization of a process that is really viscous and becomes nonlinear very rapidly. As expected, a nonlinear two-dimensional viscous calculation is necessary to obtain a really good approximation to the experimental results.

Conclusion

The first ten seconds of the formation of a methane-air diffusion flame for various Froude numbers has been simulated using the low Mach number form of the Navier-Stokes equation. The chemistry part of the calculations is modeled by the flamelet method. This avoids solving the energy and species equations for which one needs to resolve chemical time scales that are much smaller than the characteristic fluid time scale. The use of a flamelet library permits the calculations to be carried out efficiently

The natural flickering frequency of the diffusion flame for a 1 g gravitational force has been correctly predicted. It is observed that the frequency varies as $Fr^{-0.56}$. The instantaneous and time-averaged emission indexes EI_{NOX} and EI_{CO} are also determined in this study. The mass fraction of NO and NO_2 are obtained by solving the rate equations with the production rates

provided by the flamelet library. The CO mass fraction is obtained by using the flamelet data. With the increase in buoyancy force that leads to more intense flame stretching, a reduction of NO_X emission with an increase of CO emission was found. Further analysis indicates that the emission index of NO_X is proportional to $Fr^{0.21}$ while the emission index of CO is proportional to $Fr^{-1.0}$. For all cases in this study, the instantaneous EI_{NOX} and EI_{CO} are in phase.

An analysis of the instability that gives rise to the flicker of laminar diffusion flames such as the one studied here has been presented. It is capable of providing a rough estimate of the frequency of the flicker, and of the variation of the frequency with the gravitational force that helps to drive the instability. This analysis is necessarily crude; for quantitative calculations of the flickering behavior, the fully nonlinear simulation is required.

Acknowledgments

Many thanks are due M. L. Koszykowski, R. C. Armstrong, and F. P. Tully for helpful discussions and encouragement.

References

[1] Yam, C., "A study of a Turbulent Diffusion Boundary Layer Flame," Master's Thesis, U.C. Davis, 1986.

[2] Peters, N., "Laminar Diffusion Flamelet Models In Non-Premixed Turbulent Combustion," Prog. Energy Combustion Sci. **10**, pp. 319-339, 1984.

[3] Katta, V. R., Goss, L. P. and Roquemore, W. M., "Numerical Investigation of Transitional H_2/N_2 Jet Diffusion Flames," AIAA J., **32**, pp. 84-94, 1994.

[4] Kaplan, C. R., Baek, S. W., Oran, E. S. and Ellzey, J. L., "Dynamics of a Strongly Radiating Unsteady Ethylene Jet," Comb. & Flame, **96**, pp. 1-21, 1994.

[5] Smyth, K. C., Harrington, J. E., Johnson, E. L. and William, M. P., "Greatly Enhanced Soot Scattering in Flickering CH_4/Air Diffusion Flames," Comb. & Flame, **95**, pp. 229-239, 1993.

[6] A. Majda, and J. A. Sethian., "The derivation and numerical solution of the equations for zero Mach number combustion," Combust. Sci. Tech., **42**, pp. 185-205, 1985.

[7] R.G. Rehm and H.R. Baum. "The equations of motion for thermally driven buoyant flows," N.B.S.J.Res., **83**, pp297-308, 1978.

[8] Kim, J. and Moin, P., "Application of a Fractional-Step Method to Incompressible Navier-Stokes Equations," J. Computational Physics **59**, pp. 308-323, 1985.

[9] Yam, C., Marx, K., Chen, J.-Y., and Chou, C.-P., "Mathematical Model for the Formation and Development of an Unsteady Laminar Methane Jet Diffusion Flame with a Clipping Mode using a Flamelet Library", Submitted to Int. J. for Numerical Methods in Fluids.

[10] Yam, C., "An Investigation of Flow Structure and Heat Transfer Characteristics of Three Dimensional Flow", Ph. D. Thesis., U. C. Davis, 1991.

[11] Barlow, R. S. and Carter, C. D., "Raman/Rayleigh/LIF Measurements of Nitric Oxide Formation in Turbulent Hydrogen Jet Flames." Comb. & Flame, **97**, 261, 1994

[12] Rokke, N.A., Hustad, J.E., Sonju, O.K., and Williams, F.A., "Scaling of Nitric Oxide Emissions from Buoyancy-Dominated Hydrocarbon Turbulent-Jet Diffusion Flames," 24th International Symposium on Combustion/The Combustion Institute, pp. 385-393 (1994).

[13] Yamashita, H., Nishioka, M., and Takeno, T., "Prediction of NO_x Emission Index of Turbulent Diffusion Flame," pp.59-67 in Lecture Notes in Physics, Edited by Buckmaster & Takeno, Springer-Verlag (1994).

[14] Hamins, A., Yang, J. C., and Kashiwagi, T., "An Experimental Investigation of the Pulsation Frequency of Flames," Twenty-Fourth Symposium (International) on Combustion, The Combustion Institute, Pittsburgh, 1992, pp. 1695-1702.

[15] Buckmaster, J., and Peters, N., "The Infinite Candle and its Stability—A Paradigm for Flickering Diffusion Flames," Twenty-First Symposium (International) on Combustion, p. 1829, The Combustion Institute, 1986.

[16] Mahalingam, S., Cantwell, B. J., and Ferziger, J. H., "Stability of low-speed reacting flows," Phys. Fluids A **3**, 1533, 1991.

[17] Drazin, P. G., and Reid, W. H., "Hydrodynamic Stability," Cambridge University Press, 1981.

Figure Captions:

Figure 1. Maximum Temperature Location At the Center Line at 1g.

Figure 2. Emission Index for NO_X at 1 g.

Figure 3. Emission Index for CO at 1 g.

Figure 4. Flickering frequency as a function of Fr.

Figure 5. Emission indexes for NO_X and CO as a function of Fr.

Figure 6. Mean and Conditional scalar dissipation rates as a function of Fr.

Figure 7. Contour plot of vorticity at a typical time in the oscillation cycle.

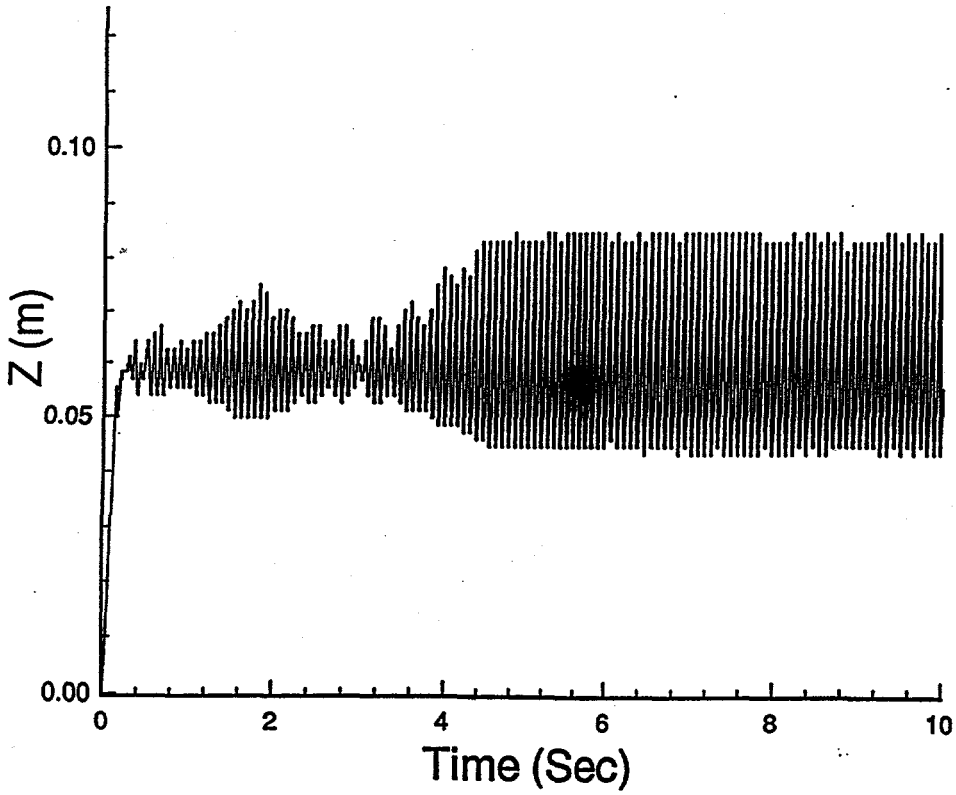

Figure 1
Maximum Temperature Location At the Center Line at 1g.

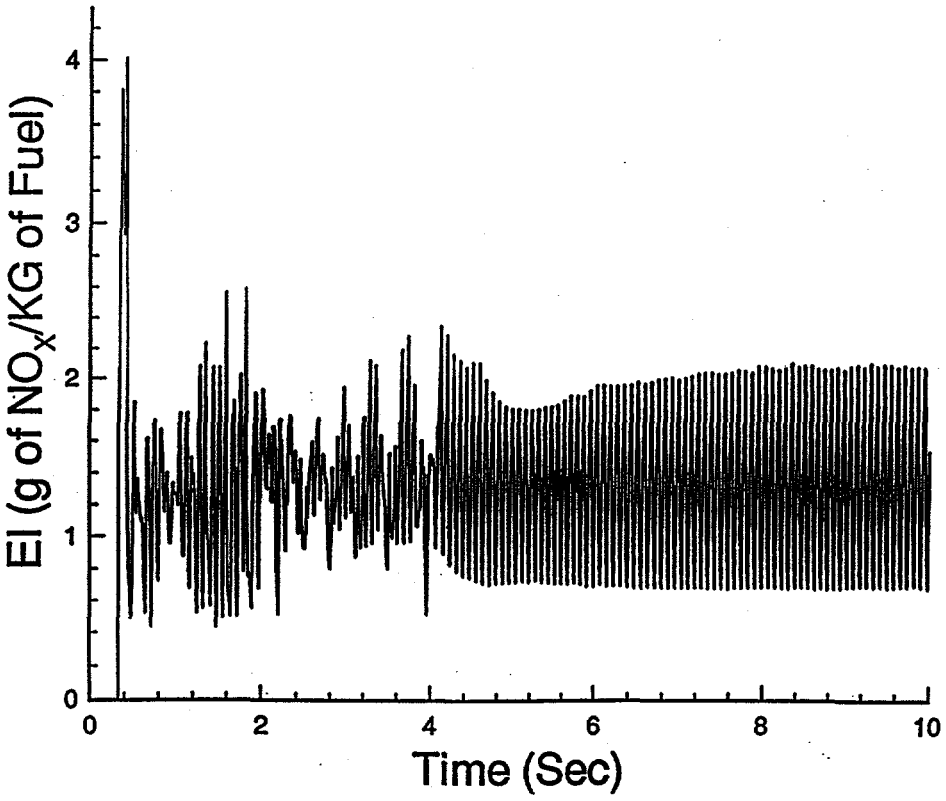

Figure 2
Emission Index for NO_X at 1 g.

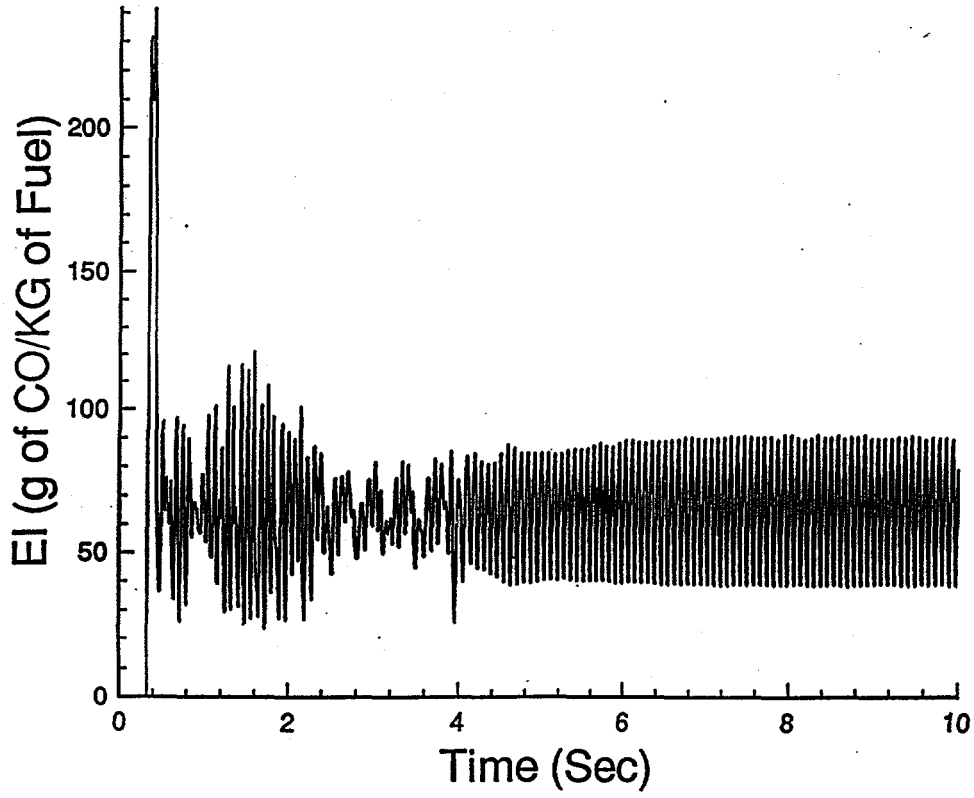

Figure 3
Emission Index for CO at 1 g.

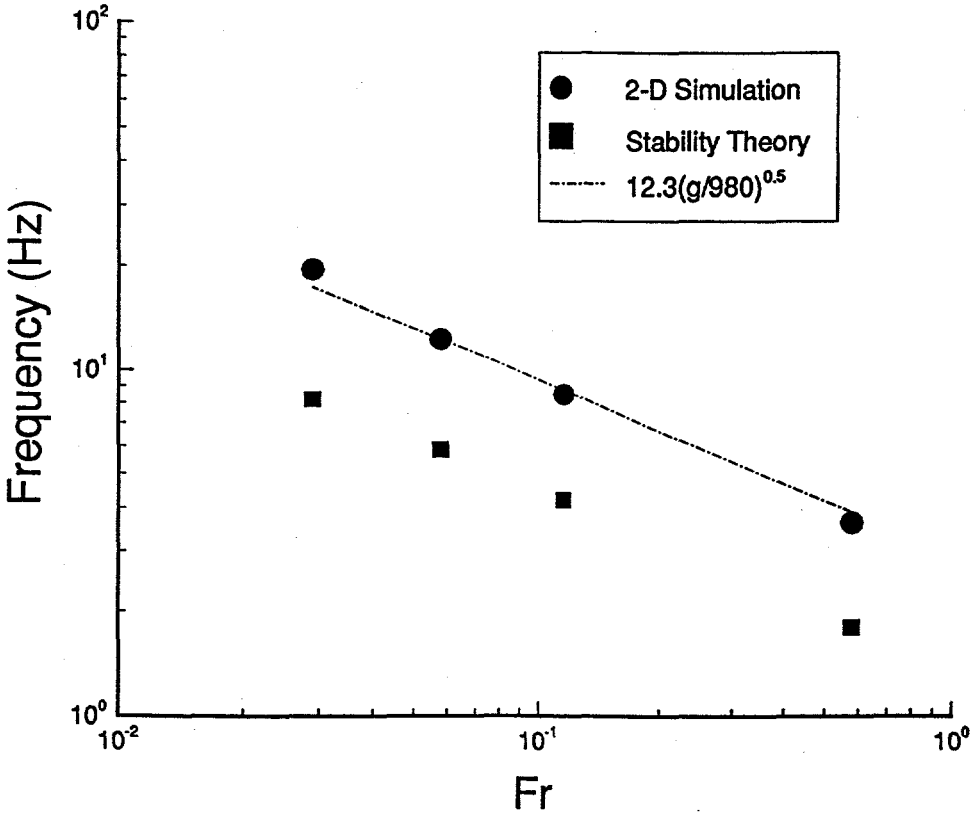

Figure 4
Flickering frequency as a function of Fr.

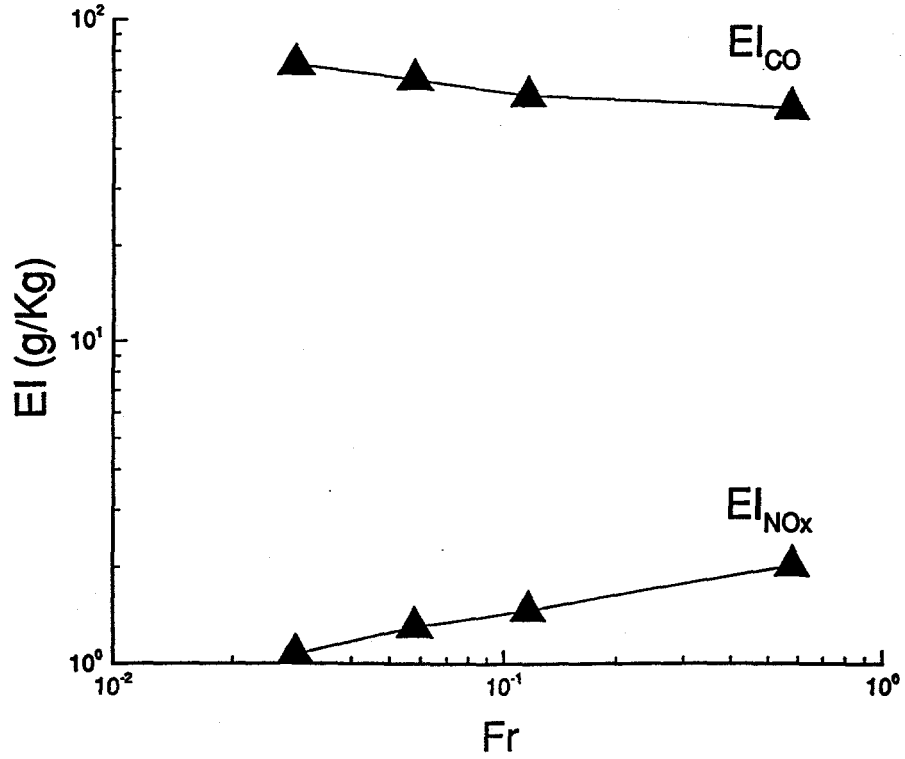

Figure 5
Emission indexes for NO_X and CO as a function of Fr.

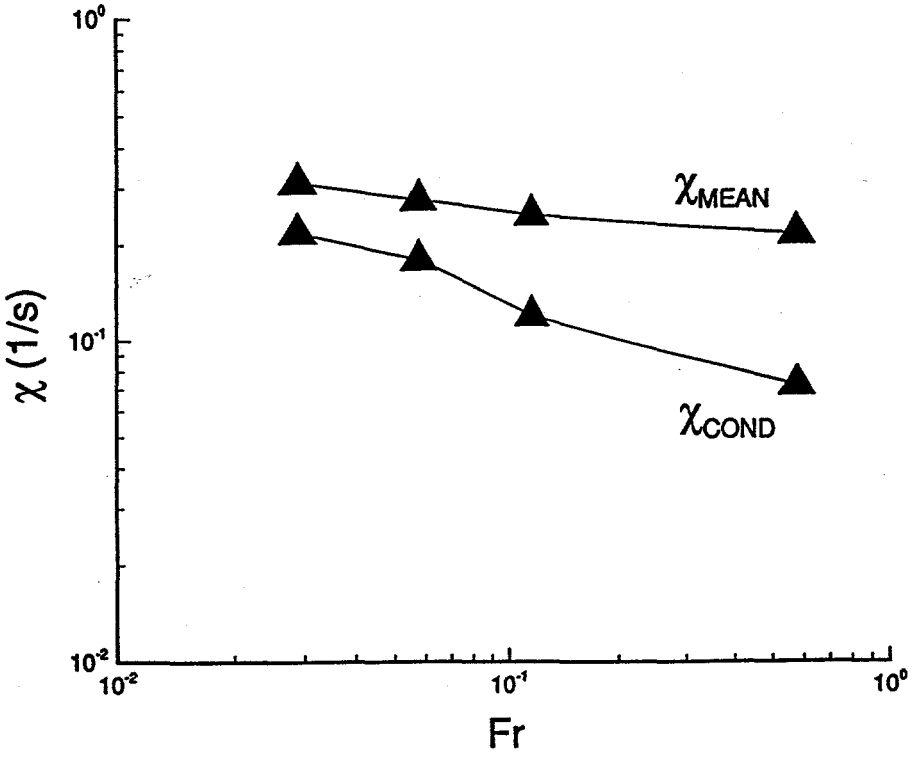

Figure 6
Mean and Conditional scalar dissipation rates as a function of Fr.

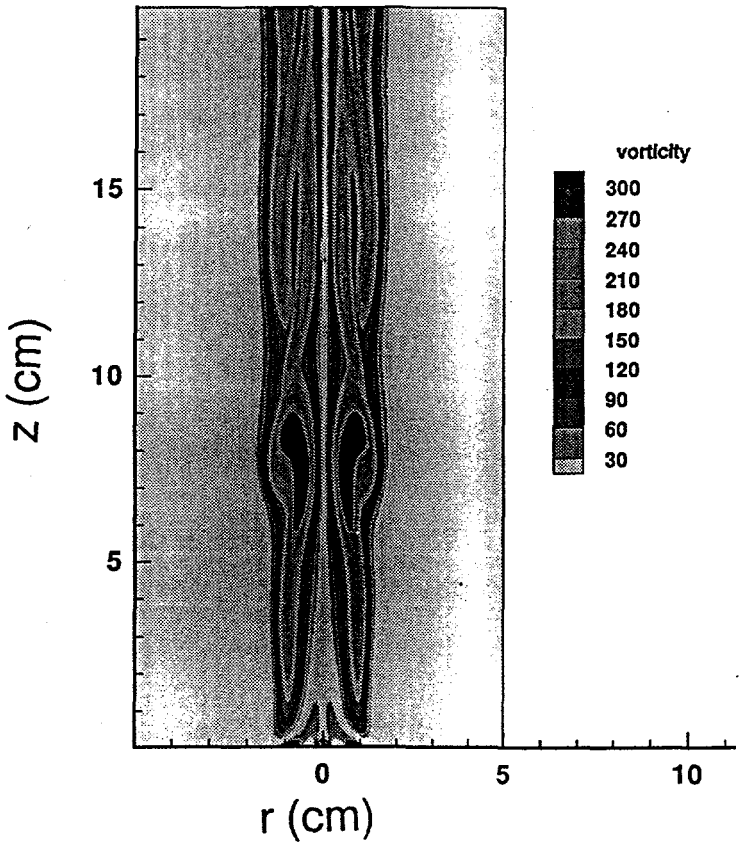

Figure 7
Contour plot of vorticity at a typical time in the oscillation cycle.